Articles

Crystal Forms of Hexafluorophosphate Organometallic Salts and the Importance of Charge-Assisted C−H---F Hydrogen Bonds

Fabrizia Grepioni,*[,†] Gianna Cojazzi,[‡] Sylvia M. Draper,[§] Noelle Scully,[†] and Dario Braga*[,†]

Dipartimento di Chimica G. Ciamician and Centro CNR per lo Studio della Fisica delle Macromolecole, c/o Dipartimento di Chimica G. Ciamician, Università di Bologna, Via Selmi 2, 40126 Bologna, Italy, and Chemistry Department, Trinity College, Dublin 2, Ireland

Received July 31, 1997[⊗]

Architecture, stability, and behavior with temperature of the hexafluorophosphate salts $[(C_5H_5)_2Co][PF_6]$ (**1**), $[(C_5H_5)_2Fe][PF_6]$ (**2**), $[(C_6H_6)_2Cr][PF_6]$ (**3**), and $[(C_6H_5Me)_2Cr][PF_6]$ (**4**) have been investigated. Crystals **1** and **2** have been measured by variable-temperature X-ray diffraction and differential scanning calorimetry. The phase-transitional behavior of $[(C_5H_5)_2Co][PF_6]$, which undergoes two fully reversible crystal-to-crystal phase transitions, has been compared with the known behavior of $[(C_5H_5)_2Fe][PF_6]$. The room- and low-temperature phases (form I and form II) of $[(C_5H_5)_2Fe][PF_6]$ and $[(C_5H_5)_2Co][PF_6]$ are isostructural and isomorphous. The basic packing features of crystalline **1** and **2** are maintained on substituting the metallocene system with the bisbenzenechromium cation in **3**. The architecture common to the three salts is otherwise disrupted by substituting toluene for benzene in **4**. It has been shown that, when assisted by the difference in charge between anions and cations, the C−H---F interactions play a significant role. The structural parameters obtained for C−H---F interactions in **1**−**4** have been compared with data retrieved from the Cambridge Crystallographic Database on interactions of the $X-H---F^{(\delta-)}$ type (X = C, N, O) in organometallic salts of the PF_6^- anion.

Introduction

Modern crystal engineering, namely the rational design of solid materials with predefined arrangements of the component molecules or ions, is a most attractive field of research.[1] Though born in the field of organic chemistry, crystal engineering now represents an extremely promising source of new discoveries as well as a fundamental scientific challenge in the neighboring areas of inorganic and organometallic chemistry. The implications of utilizing the structural and electronic features of metal atoms in preparing novel materials are enormous.[2] In this respect, it is important to be able to understand the factors responsible for cohesion and behavior with temperature of inorganic and organometallic solids. To this task we have devoted much of the research efforts carried out in Bologna over the past few years. Our attention has been focused in particular on establishing analogies and differences between intermolecular or interionic interactions at work in organometallic and organic crystals. In collaboration with others, we have shown, for example, that while all strong hydrogen-bond-donor and -acceptor groups behave essentially in the same way whether belonging to organic or organometallic molecules, this is not so when weaker interactions are involved. Besides the fascinating consequences of the direct participation of the metal atoms in intermolecular interactions, we have shown that hydrogen bonds such as C−H---O may have a crucial effect on crystal cohesion when reinforced by the different polarity of donors and acceptors, i.e., when these weak electrostatic interactions are "charge assisted".[4]

In many cases there is no unique solution to the problem of crystal cohesion as manifested by the phe-

[†] Dipartimento di Chimica G. Ciamician.
[‡] Centro CNR per lo Studio della Fisica delle Macromelecole.
[§] Trinity College.
[⊗] Abstract published in *Advance ACS Abstracts,* December 15, 1997.

(1) (a) Desiraju, G. R. *Organic Solid State Chemistry*; Elsevier: Amsterdam, 1987. (b) Desiraju, G. R. *Crystal Engineering: The Design of Organic Solids*; Elsevier: Amsterdam, 1989.

(2) (a) Braga, D.; Grepioni, F. *Acc. Chem. Res.* **1994**, *27*, 51. (b) Burrows, A. D.; Chan, C.-W.; Chowdry, M. M.; McGrady, J. E.; Mingos, D. M. P. *Chem. Soc. Rev.* **1995**, 329. (c) Subramanian, S.; Zaworotko, M. J. *Coord. Chem. Rev.* **1994**, *137*, 357. (d) Braga, D.; Grepioni, F. *J. Chem. Soc., Chem. Commun.* **1996**, 571. (e) Braga D., Grepioni, F., Desiraju, G. R. *Chem. Rev.*, submitted.

(3) (a) Braga, D.; Grepioni, F.; Sabatino, P.; Desiraju, G. R. *Organometallics* **1994**, *13*, 3532. (b) Braga, D.; Grepioni, F.; Tedesco, E.; Biradha, K.; Desiraju, G. R. *Organometallics* **1997**, *16*, 1846 and references therein.

S0276-7333(97)00662-6 CCC: $15.00
Publication on Web 01/07/1998

nomenon of crystal polymorphism.[5] In the presence of polymorphism, the relationship between intermolecular interactions and crystal stability becomes intriguing. Polymorphism is related to the phase-transitional behavior of the crystalline material depending on whether the polymorphic modifications belong to enantiotropic systems (*i.e.*, the solid−solid transition between polymorphs is below the solid−liquid transition and the polymorphs interconvert before melting) or to monotropic systems (*i.e.*, the polymorphs melt before the solid−solid transition can occur). In a supramolecular approach, the change in crystal structure associated with a phase transition, in which intermolecular noncovalent bonds are broken and formed, is the *solid-state* equivalent of an isomerization at the molecular level. Since chemical and physical properties of the crystalline material can change dramatically with the solid-state transformations, it would be highly desirable to be able to understand the relationship between noncovalent interactions and cohesion of the polymorphic phases.

Many crystals of globular organometallic molecules have been shown to undergo phase transitions, and, in some cases, the presence of plastic phases is known. These are characterized by short-range orientational disorder and long-range order. For instance, the substituted ferrocene derivatives $[(C_5H_5)(C_5H_4CHO)Fe]$[6a] and $[(C_5H_5)(C_5H_4CMeO)Fe]$[6b] as well as salts of the type [(FC$_6$H$_5$)(C$_5$H$_5$)Fe][counterion] (counterion = AsF_6, PF_6, SbF_6, and BF_4)[6a,c] are all known to undergo order−disorder phase transitions. The transition from the ordered phase to a disordered one is usually associated with the onset of reorientational motion of the molecules or ions.[6]

In this paper, we will discuss crystal structure and phase transitional behavior of the metallocene complexes $[(C_5H_5)_2M][PF_6]$ (M = Co, **1**; Fe, **2**] and of the bisarene complexes $[(arene)_2Cr][PF_6]$ (arene = benzene, **3**; toluene, **4**] that have all been crystallized as hexafluorophosphate salts. Crystalline $[(C_5H_5)_2Fe][PF_6]$[7a,b] **2** was known to undergo a phase transition from a monoclinic crystal to a plastic cubic phase at 347 K.[7b] Both phases were characterized by single-crystal X-ray diffraction and investigated by ^{2}H NMR and ^{57}Fe Mössbauer techniques. Calorimetric measurements had also indicated that a second phase transition occurs on cooling the crystal below 210 K,[7c] but the crystal structure of the low-temperature phase was not determined. The phase-transitional behavior of crystalline $[(C_5H_5)_2Co][PF_6]$ has been the subject of a preliminary communication.[8]

The discussion will be organized as follows:

(i) The relationship between the three phases of crystalline $[(C_5H_5)_2Co][PF_6]$ (**1**) (form I at room temperature, form II at 243 K, form III at 323 K) will be discussed. New information concerning the high-temperature phase will be added to those previously communicated.[8]

(ii) The crystal-packing and phase-transition behavior of $[(C_5H_5)_2Co][PF_6]$ will be compared with that of $[(C_5H_5)_2Fe][PF_6]$ (**2**). The room-temperature structure of **2** has been determined previously and independently by two groups[7a,b] and is isomorphous with that of **1**. The crystal structure of the low-temperature phase of crystalline $[(C_5H_5)_2Fe][PF_6]$, not known before, has been determined and will be used in the comparison. The high-temperature phase transition of $[(C_5H_5)_2Fe][PF_6]$ has been measured by DSC, and data will be compared with those available in the literature.[7c]

(iii) Crystals of the PF_6^- salts of $[(C_6H_6)_2Cr]^+$ (**3**) and of $[(C_6H_5Me)_2Cr]^+$ (**4**) have also been obtained and characterized. Analogies and differences with crystals **1** and **2** will be discussed.

(iv) Finally, the role played by C−H---F interactions will be discussed. The results obtained from the comparative analysis of the hexafluorophosphate salts **1**−**4** will be put in the broader perspective of a Cambridge Crystallographic Database investigation of the occurrence of X−H---F bonds (X = C, N, O) involving the hexafluorophosphate anion.

Experimental Section

Synthesis of Crystalline $[(C_5H_5)_2Co][PF_6]$. $[(C_5H_5)_2Co]$ purchased from Aldrich (100 mg, 0.529 mmol) was dissolved in acetonitrile and treated with HCl(aq). From the yellow solution crystals of $[(C_5H_5)_2Co][PF_6]$ were precipitated almost quantitatively by addition of $[NH_4][PF_6]$ (90 mg, 0.552 mmol). The yellow crystals are stable in the air and in the mother liquor.

Synthesis of $[(C_6H_6)_2Cr][PF_6]$. Brown crystalline $[(C_6H_6)_2Cr]$ purchased from Strem (48 mg, 0.231 mmol) was added to a flask containing distilled water (5 mL). The mixture was stirred until complete dissolution accompanied by the appearance of a bright yellow color indicating complete oxidation to $[(C_6H_6)_2Cr]^+$. To this solution was added $[NH_4][PF_6]$ (40 mg, 0.245 mmol), and a yellow precipitate was obtained. After filtration, the solid residue was dissolved in acetonitrile. Slow evaporation of the solvent afforded crystals suitable for X-ray diffraction.

Synthesis of $[(C_6H_5Me)_2Cr][PF_6]$. $[(C_6H_5Me)_2Cr]$ prepared according to the literature[9] (60 mg 0.254 mmol) was dissolved in distilled water (5 mL) and oxidized by oxygen bubbled through the solution. To this solution was added

(4) (a) Braga, D.; Scaccianoce, L.; Grepioni, F.; Draper, S. M. *Organometallics* **1996**, *15*, 4675. (b) Braga, D.; Grepioni, F.; Byrne, J. J.; Wolf, A. *J. Chem. Soc., Chem. Commun.* **1995**, 1023. (c) Braga, D.; Costa, A. L.; Grepioni, F.; Scaccianoce, L.; Tagliavini, E. *Organometallics* **1996**, *15*, 1084.

(5) Gavezzotti, A. *Acc. Chem. Res.* **1994**, *27*, 309. Dunitz, J.; Bernstein, J. *Acc. Chem. Res.* **1995**, *28*, 193 and references therein.

(6) (a) Daniel, M. F.; Leadbetter, A. J.; Meads, R. E.; Parker, W. G. *J. Chem. Soc., Faraday Trans.* **1978**, *74*, 456. (b) Sato, K., Katada, M.; Sano, H.; Konno, M. *Bull. Chem. Soc. Jpn.* **1984**, *57*, 2361. (c) Fitzsimmons, B. W.; Sayer, I. *J. Chem. Soc., Dalton Trans.* **1991**, 2907.

(7) (a) Martinez, R.; Tiripicchio, A. *Acta Crystallogr. Sect. C* **1990**, *C46*, 202. (b) Webb, R. J.; Lowery, M. D.; Shiomi, Y.; Sorai, M.; Wittebort, R. J.; Hendrickson D. N. *Inorg. Chem.* **1992**, *31*, 5211. (c) Sorai, M.; Shiomi, Y. *Thermochimica Acta* **1986**, *109*, 29.

(8) (a) Braga, D.; Scaccianoce, L.; Grepioni, F.; Draper, S. M. *Organometallics* **1996**, *15*, 4675. (b) Some readers may be concerned by the quality of the diffraction data obtained for form II of **2** and for form III of **1**. The overall quality of X-ray data collected on organometallic crystals that undergo two-phase transitions within a small temperature interval cannot be compared with those obtainable with normal, well-behaving, crystals. Crystalline **1** and **2** are not polymorphs that can be separately treated: the only way to collect data on the low- and high-temperature phases is by having the crystals undergo phase transition on the diffractometer starting from the room temperature phases. Though reversible, the phase transitions cannot be expected to leave the crystals unaffected.

(9) Calderazzo, F.; Invernizzi, R.; Marchetti, F.; Masi, F.; Moalli, A.; Pampaloni, G.; Rocchi. L. *Gazz. Chim. Ital.* **1993**, *123*, 53.

Table 1. Thermodynamic Data for the Phase Transitions of Crystalline 1 and 2

	T (K) form I ⇔ form II	T (K) form I ⇔ form III	ΔH (kJ·mol^{-1}) form I ⇔ form II	ΔH (kJ·mol^{-1}) form I ⇔ form III	mp (K)
1	251.77[a]	313.86[a]	1.27[a]	3.06[a]	417.15
	239.09[b]	309.31[b]	1.34[b]	3.05[b]	
2		347.10[a]		4.50[a,b]	
		340.62[b]	1.95[c]	4.84[c]	
	213.05[c]	346.94[c]			

[a] DSC, heating. [b] DSC, cooling. [c] Calorimetric studies.[7c]

$[NH_4][PF_6]$ (42 mg, 0.258 mmol), and a yellow precipitate was obtained. After filtration, the solid residue was dissolved in THF. The yellow THF solution was then placed in a test tube, and toluene was slowly added dropwise; crystals suitable for X-ray diffraction were obtained *via* slow diffusion of the two solvents.

Differential Scanning Calorimetry (DSC). DSC thermograms of compounds **1** and **2** were measured on a Perkin-Elmer DSC-7 in sealed Al-pans. **1**: 5.150 mg of crystalline material was taken from the same crystal batch used for the diffraction experiments. Repeated cycles of cooling and heating (scanning rate 5.0 deg/min) had hystereses of 12.7 and 4.5 K for the form I ⇔ form II and the form I ⇔ form III transitions, respectively. **2**: 8.030 mg of crystalline material was taken from the same crystal batch used for the diffraction experiments. Repeated cycles of cooling and heating (scanning rate 5.0 deg/min) had hysteresis of 6.48 °C for the form I ⇔ form III transition. The low-temperature phase transition could not be observed, as 213 K was the minimum temperature reachable with the instrument used for the measurements.

Crystal Structure Determination. Crystals of compound **3** and **4** are rapidly decomposed if exposed to air under the X-ray beam. Data sets at low temperature for these species were thus collected from crystal specimens covered with inert glue (**3**) or sealed in a glass capillary together with some THF solution (**4**). Diffraction intensities for compounds **1**−**4** were collected on an Enraf-Nonius CAD-4 diffractometer equipped with a graphite monochromator (Mo Kα radiation, $\lambda = 0.710\ 69$ Å). The Oxford Cryosystem device was used for the low- and high-temperature data collections. All refinements have been carried out on F^2 using all reflections. Conventional R values based on an $I > 2\sigma(I)$ cutoff are also reported for sake of comparison.

Crystal Data. 1. form III, monoclinic data collection: $C_{10}H_{10}CoF_6P$, $M = 334.08$, monoclinic, space group $P2_1/c$, $a = 13.426(5)$ Å, $b = 9.518(5)$ Å, $c = 9.505(5)$ Å, $V = 1215(1)$ Å^3, $Z = 4$, $T = 323(2)$ K, $d_c = 1.827$ g cm^{-1}, $\mu = 1.597$ mm^{-1}, 2534 reflections measured, refinement on F^2 (1550 independent reflections) for 142 parameters; wR(F^2 all) = 0.382, R_1(466 reflections with $I > 2\sigma$(I)) = 0.096, $S = 0.938$; crystal size 0.16 × 0.14 × 0.14 mm, F(000) = 664; θ-range 3.0−23.0°. Crystal data concerning the room-temperature (form I), low-temperature (form II), and form III data collection in the cubic setting are available in ref 8. Altogether, the experiments on crystals of **1** were repeated seven times on four different crystals to check reproducibility and to obtain the best possible set of diffraction data for publication.[8b]

2. Form II: $C_{10}H_{10}FeF_6P$, $M = 331.00$, monoclinic, space group $P2_1/c$, $a = 13.431(10)$ Å, $b = 9.268(4)$ Å, $c = 9.328(7)$ Å, $V = 1153(1)$ Å^3, $Z = 4$, $T = 143(2)$ K, $d_c = 1.907$ g cm^{-1}, $\mu = 1.503$ mm^{-1}, 1457 reflections measured, refinement on F^2 (1198 independent reflections) for 148 parameters; wR(F^2 all) = 0.386, R_1 (642 reflections with $I > 2\sigma(I)$) = 0.124, $S = 1.140$; crystal size 0.12 × 0.10 × 0.10 mm, F(000) = 660; θ-range 3.0−28.0°.[8b] Structural data for form I and form III for **2** are obtained from ref 7b.

3: $C_{12}H_{12}CrF_6P$, $M = 354.18$, orthorhombic, space group $Pna2_1$, $a = 9.587(6)$ Å, $b = 9.661(4)$ Å, $c = 27.510(10)$ Å, $V = 2548(2)$ Å^3, $Z = 8$, $T = 143(2)$ K, $d_c = 1.841$ g cm^{-1}, $\mu = 1.081$ mm^{-1}, 4190 reflections measured, refinement on F^2 (3753 independent reflections) for 316 parameters; wR(F^2 all) = 0.158, R_1(1729 reflections with $I > 2\sigma(I)$) = 0.048, $S = 1.065$; crystal size 0.14 × 0.15 × 0.08 mm, F(000) = 708; θ-range 3.0−30.0°. Absolute structure parameter = 0.10(11).

4: $C_{14}H_{16}CrF_6P$, $M = 381.24$, monoclinic, space group $P2_1/n$, $a = 6.793(2)$ Å, $b = 11.056(2)$ Å, $c = 10.740(5)$ Å, $V = 779.2(5)$ Å^3, $Z = 2$, $T = 273(2)$ K, $d_c = 1.625$ g cm^{-1}, $\mu = 0.891$ mm^{-1}, 1167 reflections measured, refinement on F^2 (1028 independent reflections) for 93 parameters; wR(F^2 all) = 0.139, R_1(672 reflections with $I > 2\sigma(I)$) = 0.045, $S = 1.087$; crystal size 0.16 × 0.12 × 0.10 mm, F(000) = 772; σ-range 3.0−25.0°.

The computer programs SHELX86[10a] and SHELXL92[10b] were used for structure solution and refinement. All atoms except the hydrogen atoms and the C atoms in **1** (form III) were treated anisotropically. Hydrogen atoms were added in calculated positions and refined riding on their respective C atoms. No attempt to model H-atom positions in the high temperature form III was made. For all molecular representations the graphic program SCHAKAL92[10c] was used. The program PLATON[10d] was used to calculate the hydrogen-bonding interactions of the C−H---F type. For these calculations all C−H distances were normalized to the neutron-derived value (1.08 Å). Crystal data and details of measurement, tables of atomic coordinates, tables of anisotropic thermal parameters, and tables of bond lengths and angles are all available as Supporting Information and have been deposited with the Cambridge Crystallographic Data Centre.

Intermolecular Searches of X−H---F (X = C, N, O) Interactions. Searches were made with version 5.13 of the CSD[10e] (April 1997), by using the program QUEST3D,[10f] on organometallic salts containing at least one transition metal atom and one PF_6^- anion. Structures affected by disorder or for which no coordinates of the H atoms were available were excluded. Intermolecular contacts of the X−H---F type (X = C, N, O) with H---F distances less than 2.6 Å and X−H---F angles greater than 90° were accepted and subsequently examined with the VISTA package.[10f] X−H distances were all normalized to the neutron-derived values (1.080 Å for C−H, 1.009 Å for N−H, 0.983 Å for O−H).

Results and Discussion

Phase Transitions in $[(C_5H_5)_2Co][PF_6]$ (1) and in $[(C_5H_5)_2Fe][PF_6]$ (2). In view of the strict analogies between structure and behavior with temperature of crystalline **1** and **2**, the two systems will be discussed together. Both systems undergo two phase transitions, indicated as form I ⇔ form II and form I ⇔ form III, form I being the room-temperature structure, within narrow temperature intervals. The thermodynamic

(10) (a) SHELX86: Sheldrick, G. M. *Acta Crystallogr.* **1990**, *A46*, 467. (b) SHELX92: Sheldrick, G. M. *Program for Crystal Structure Determination*; University of Göttingen, Göttingen, Germany, 1992. (c) SCHAKAL92: Keller, E. *Graphical Representation of Molecular Models*; University of Freiburg: Germany, 1992. (d) PLATON: Spek, A. L. *Acta Crystallogr. Sect. A* **1990**, *A46*, C31. (e) Allen, F. H.; Davies, J. E.; Galloy, J. J.; Johnson, O.; Kennard, O.; Macrae C. F.; Mitchell, E. M., Mitchell G. F.; Smith, J. M.; Watson, D. G. *J. Chem. Inf. Comput. Sci.* **1991**, *31*, 187. (f) CSD User Manuals; Cambridge Crystallographic Data Centre, 12 Union Road, Cambridge CB2 1EZ, U.K.

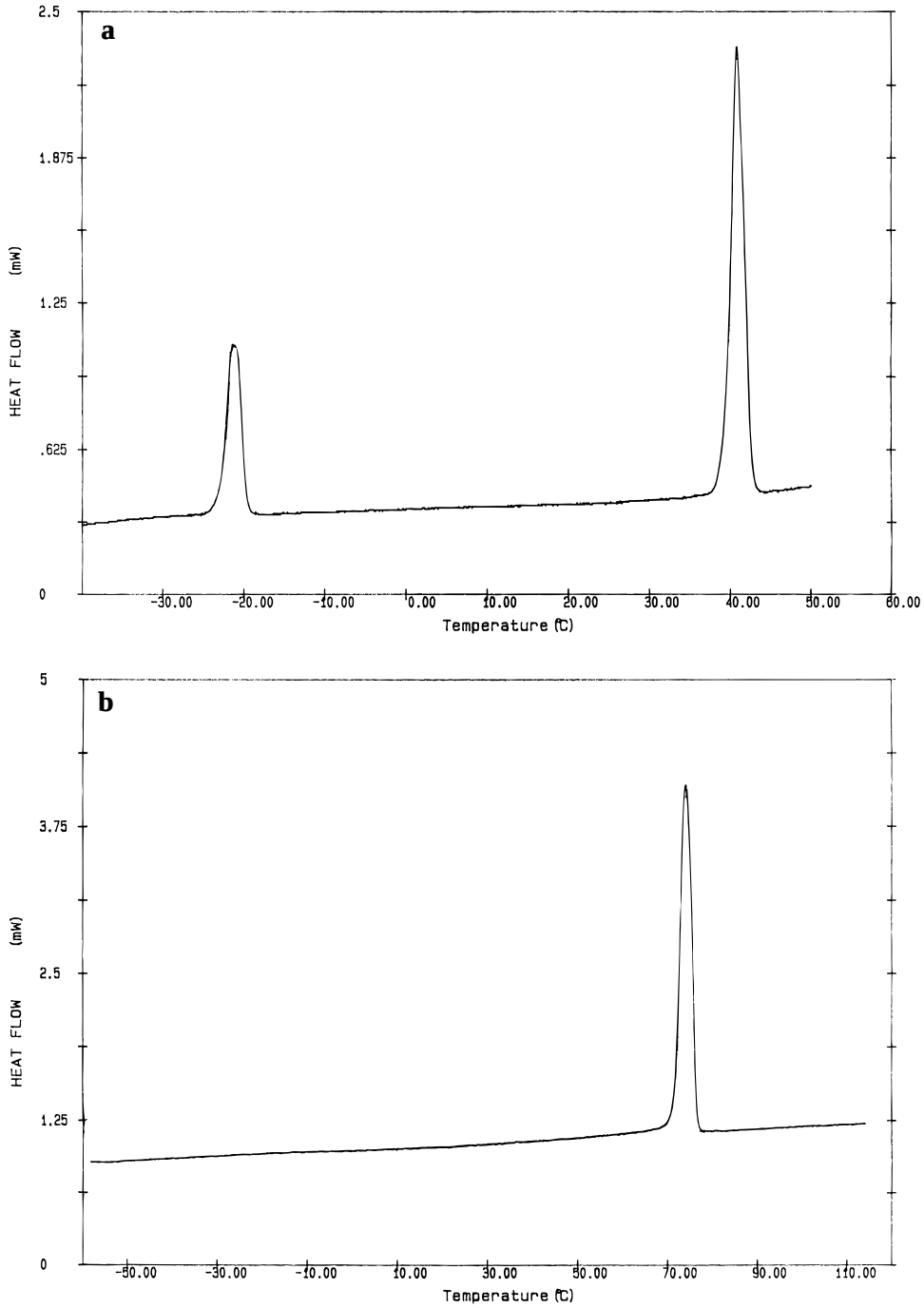

Figure 1. DSC thermograms for **1** (a) and **2** (b) showing the endothermic peaks for the orm I ⇔ form II of **1** and for the form II ⇔ form III transitions of both **1** and **2**. The form I ⇔ form II transition of **2** could not be measured for instrumental limitations (see the Experimental Section).

data are summarized in Table 1. In the case of **1**, the DSC thermograms show two endothermic peaks at 252 and at 314 K (see Figure 1a). The enthalpy differences associated with the two transitions are 1.30 and 3.05 $kJ \cdot mol^{-1}$ for the form I ⇔ form II and form I ⇔ form III phase transitions, respectively. In the case of **2**, the form I ⇔ form II transition occurs at 213 K,[7c] while the form I ⇔ form III transition occurs at 347 K (see Figure 1b). The enthalpy difference associated with this latter transition is 4.50 $kJ \cdot mol^{-1}$. The enthalpy values of these transitions fall within the range observed for most polymorphic organic crystals.[11] The DSC measurement of the low-temperature phase transition in the case of **2** was not possible because of instrumental limitations. The value given by Sorai and Shiomi[7c] in their previous thermodynamic study (see Table 1) has been used as a reference to perform the low-temperature diffraction experiment on **2**. However, the low-temperature form I ⇔ form II phase transition was observed to occur only at *ca.* 140 K on the single-crystal diffractometer, probably due to severe supercooling.

In the case of **1**, the three crystal phases have been fully characterized by single-crystal X-ray diffraction at variable temperature carried out on the *same crystal specimen*.[8b] In the case of **2** only the low-temperature crystal structure (not determined before) has been

(11) Gavezzotti, A.; Filippini, G. *J. Am. Chem. Soc.* **1995**, *117*, 12299.

Table 2. Cell Parameters, *Z*, and Packing Coefficient Values for Compounds 1−3

species	form	*a* (Å)	*b* (Å)	*c* (Å)	*β* (deg)	V_{cell} (Å^3)	*Z*	p.c.[a]	*T* (K)
1	II	13.419(7)	9.286(5)	9.343(6)	96.17(6)	1157(1)	4	0.69	243
1	I	13.355(3)	9.441(8)	9.427(6)	92.87(4)	1187(1)	4	0.67	293
1	III cubic	6.72(1)				304(1)	1		323
	III monoclinic	13.426(5)	9.518(5)	9.505(5)	90.17(4)	1215(1)	4	0.65	323
2	II	13.431(9)	9.268(4)	9.328(6)	96.91(6)	1153(1)	4	0.70	143
2 (ref. 7b)	I	13.408(6)	9.530(2)	9.482(2)	93.17(3)	1209(1)	4	0.67	299
2 (ref. 7b)	III	6.806(4)				315.3(3)	1	0.64	360
3		9.587(6)	9.661(4)	27.510(10)		2548(2)	8	0.70	203
3[b]		9.667(8)	9.712(4)	27.74(2)		2604(3)	8	0.69	293

[a] Packing coefficient was evaluated by the expression: p.c. = $[[V_{anion} + V_{cation}](Z/V_{cell})]$, where $V_{anion} + V_{cation}$ has been calculated with the integration method.[13] [b] Cell parameters at room temperature were also evaluated for compound **3**.

characterized, after the room temperature cell was determined and compared to the literature values,[7a,b] and the phase transition was observed on the diffractometer.

The room temperature form I of **1** and **2** is monoclinic ($P2_1/c$) with the unit cell containing one PF_6^- anion in a general position and two independent half-cations located on the crystallographic centers of inversion. On cooling both **1** and **2**, the form I ⇔ form II phase transition occurs, leading from the room-temperature $P2_1/c$ monoclinic cell to another $P2_1/c$ monoclinic cell with a different angle [92.87(4) and 96.17(1)°; 93.17(3) and 96.91(6)° for form I and form II of **1** and **2**, respectively] and slightly different unit cell axes (see Table 2). On passing through the phase transition the *b*- and *c*-axes shorten with respect to the room temperature cell, while the *a*-axis lengthens. The form I ⇔ form II transformation is accompanied by a change in cell volume from 1187 to 1157 Å^3 and from 1209 to 1153 Å^3 for **1** and **2**, respectively. In summary, the form I ⇔ form II phase transitions of **1** and **2** lead in both cases from an ordered monoclinic cell to another ordered cell, the only important difference being the temperature of the transition, which is 26 K lower (on cooling) in the case of **2** with respect to **1**. The form I ⇔ form II phase transition is fully reversible.[8] The relationship between the two crystal structures is depicted in Figure 2. Cations of type A (empty atom spheres), with the Cp−M−Cp molecular axes almost parallel to the *a*-axis, and of type B (filled atom spheres), with the molecular axes almost perpendicular to the *a*-axis (see Figure 2), stack along the cell *a*-axis in an A/B/A/B sequence. On going from form I to form II, the Cp−M−Cp molecular axes that are eclipsed (in projection) at room temperature become staggered at low temperature.

As shown by the calorimetric measurements (Figure 1), both **1** and **2** undergo a second phase transition at 314 and 347 K, respectively (on heating), to the crystalline form III. In the case of **1**, diffraction data of form III measured at 323 K showed fully ordered anions and orientationally disordered cations in the cubic system Pm-3.[8] In the case of **2**, the high-temperature plastic phase has also been described in the cubic system Pm-3, but with both anions and cations orientationally disordered.[7b] As in the case of the form I ⇔ form II transformation, the form I ⇔ form III transition has been demonstrated, at least in the case of **1**, to be *fully reversible* on the same crystal sample as the form I ⇔ form II transformation.[8a]

In the case of **1**, we have been able to correlate the cubic structure to the original monoclinic one, and a new data collection has been carried out for form III in the monoclinic system. The purpose of this new experiment on **1** was that of gaining insight into the phase-transition mechanism by checking whether form III could be described in a system of lower symmetry that retained the two independent crystallographic sites for the two cations. This idea arises from the observation

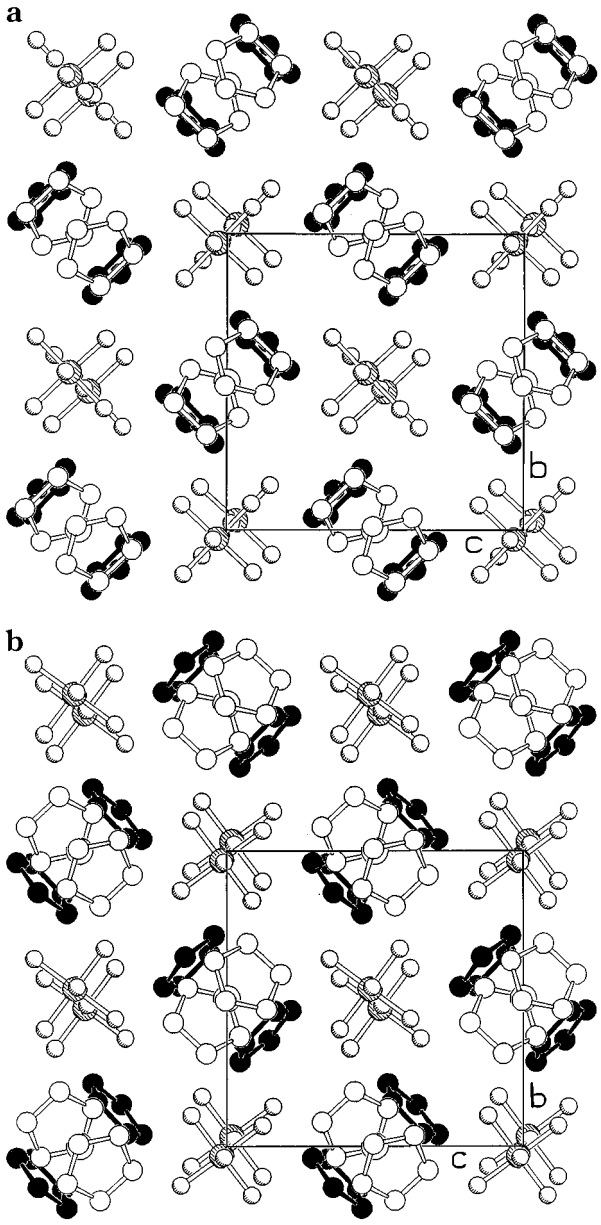

Figure 2. Schematic representation of the form I ⇔ form II phase transition: the Cp−M−Cp molecular axes that at room temperature are eclipsed (in projection) (a) become staggered at low temperature (b).

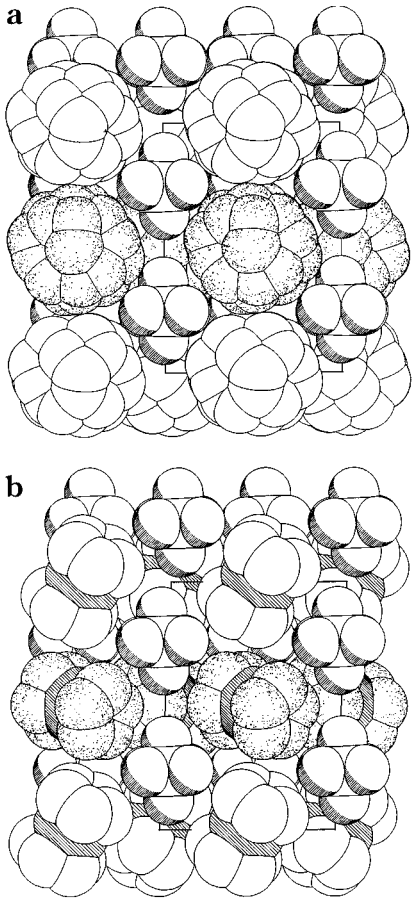

Figure 3. Space-filling representation in the *ac*-plane of the form III disorder monoclinic structure (a) and of the ordered form II structure of **1**. Note how the centers of mass of the cations and the anions do not "move" upon crystal transformation, while the Cp-ligands appear to rotate around the metal centers to the disordered arrangement.

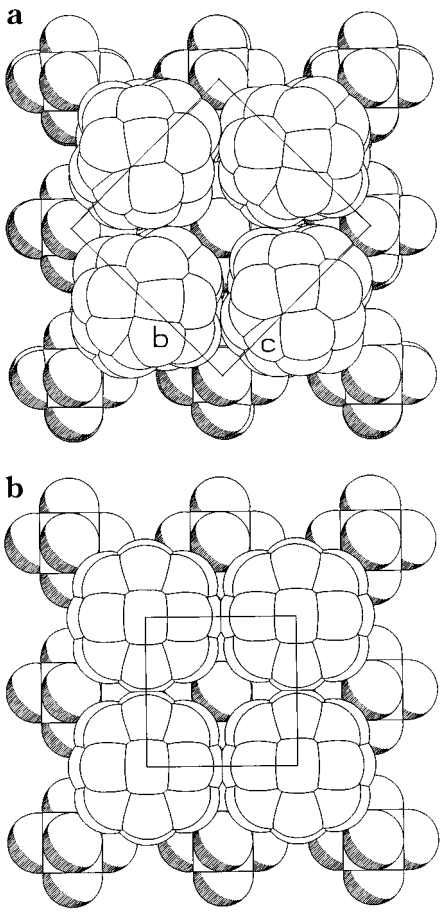

Figure 4. Space-filling projections of form III in the monoclinic (this paper) and cubic (ref 8) settings. Note the relationship between the monoclinic (corners occupied by PF_6^- anions) and the cubic cells (corners occupied by disordered cobalticinium cations).

that the transformation from low temperature to high temperature is accompanied by a progressive change of the monoclinic cell with the monoclinic angle "clicking" from 96.17(6) to 92.87(4) to 90.17(4)° as the transformation proceeds *via* the form II → form I and form I → form III transitions (see Table 2). This latter "click" is associated with the onset of what appears to be an almost random disordering of the Cp-ligands around the cobalt centers, which do not change position. A space-filling representation in the *ac*-plane of the disorder in form III of **1** is shown in Figure 3a and compared with a space-filling view of form II in the same orientation (Figure 3b).

Unfortunately (though expectedly[8b]), the high-temperature data sets are affected by a severe loss of diffraction power. Only few hundred reflections are measurable at 323 K, and the limited number of reflections reduces the resolution, which is a serious drawback in the presence of disorder. Nonetheless, we have been able to locate peaks in the Fourier maps that correspond to the fraction of carbon atoms with site occupancy factors ranging from 0.60(5) to 0.10(5). Altogether, the fractions of carbon atoms account satisfactorily for as much as 98.4% of the expected electron density. Space-filling projections of form III in the monoclinic (this paper) and cubic (ref 8) settings are compared in Figure 4.

The cubic cell, then, results from the average *over space* of the two cobalticinium cation sites. A way to depict it is as follows: as the temperature increases the librational motion of the ligands requires more space; hence, the "box" (defined by the PF_6^- anions) in which the cobalticinium cation is encapsulated becomes larger and, on average, more isotropic (*i.e.*, closer to the cubic symmetry). There is no way to tell with confidence from the high-temperature diffraction data whether the dynamic disordering of the Cp ligands makes the two sites identical also *over time*. One of the questions behind the observation of such a fully reversible order-to-disorder phase transition is that related to the degeneracy of the process. One has to (or, at least, has to try to) explain how possibly the (apparent) degeneracy of the high-temperature phase with metallocenium cations in random orientations in both **1** and **2** disappears on cooling. The diffraction experiments show that (even after a long heating, *ca*. 24 h, at 323 K) the ordered monoclinic structure is fully restored though with a loss of diffraction power. These observations may suggest that *form III is cubic only on average over space but remains monoclinic on average over time*. Within this hypothesis the orientational disorderings of the two independent cations in the high-temperature phase are not degenerate, allowing the Cp ligands to revert, on cooling, to the original sites of lower energy. In view of the paucity of available experimental data, this conclu-

sion is admittedly speculative. Some support, however, derives from the observation that when treated in the monoclinic setting at high temperature the cell of **1** refines to slightly different values of the *b*- and *c*-axes (see Table 2) and that the monoclinic β angle is slightly different from 90°.

Crystal Structure of the PF_6^- Salts of $[(C_6H_6)_2Cr]^+$ (3) and of $[(C_6H_5Me)_2Cr]^+$ (4). On changing the 5-fold symmetry of the metallocene cations of **1** and **2** to the 6-fold symmetry of the benzene ligands of **3**, the crystal architecture is essentially retained unchanged. The relationship between the monoclinic unit cells of **1** and **2** and that of **3** is clear to see (Table 2): *a* (**1**, **2** monoclinic) $\approx$ *b* (**3**) , *b* (**1**, **2** monoclinic) $\approx$ *c* (**3**), *c* (**1**, **2** monoclinic) $\approx 2a$ (**3**).

The fact that the three crystals are *quasi*-isomorphous, in spite of the structural differences between the organometallic cations, lends further support to the idea that objects of similar shape tend to pack in a similar manner, provided that the type of noncovalent interactions at work are not significantly altered.[12] A space-filling representation of the crystal structure of **3** is compared with the corresponding orientation of the crystal structure of **1** (form II) in Figure 5.

In addition to this structural analogy there are some important features that need to be discussed. Although constructed of centrosymmetric bis-benzenechromium cations and of centrosymmetric hexafluorophosphate anions, compound **3** crystallizes in the *polar* space group $Pna2_1$, with two independent $[(C_6H_6)_2Co]^+$ cations and PF_6^- anions in the asymmetric unit. The benzene ligands are in eclipsed conformation in both cations, as usually observed for bis-benzene transition metal complexes. The two independent cations in **3** have the *same relative arrangement* observed in the low-temperature phases of **1** and **2** (form II); *i.e.*, the cation molecular axes are staggered in projection (see Figure 6). However, the stacking sequence now is not A/B/A but A/B/A′/B′/A/B, where the orientation of the cations A′ and B′ with respect to that those of type A and B is related by the crystallographic 2_1-axis. This decreases the periodicity and doubles the cell *c*-axis with respect to the cell *a*-axes of **1** and **2** (see Table 2).

Table 2 allows a comparison of the packing coefficients (p.c.),[13] *i.e.*, of the efficiency of volume occupation in the various forms of **1**, and **2** with crystalline **3**. It is worth noting that the p.c. values vary from 0.69 to 0.65 and from 0.70 to 0.64 on warming crystals **1** and **2**, respectively. These changes reflect a substantial decrease of the crystal density as the temperature is raised in keeping with the "plasticity" of the systems. Importantly, crystal **3**, which retains the same packing arrangement on cooling, undergoes a much smaller p.c. change with temperature (from 0.69 to 0.70).

The compound $[(C_6H_5Me)_2Cr][PF_6]$ (**4**) crystallizes in the monoclinic space group $P2_1/n$. Both cation and anion lie on crystallographic centers of inversion. The two toluene ligands are staggered with respect to the methyl groups; this is the conformation observed in most bis-toluene complexes, probably because it minimizes the steric repulsions between the methyl ligands. The presence of a methyl on the arene ligands disrupts the 6-fold symmetry of the cation and prevents a packing arrangement similar to the one observed for the bis-benzene analogue. The crystal is constituted of columns of cations extending along the *a*-direction. The columns of cations are in close contact; the anions also form columns along the same direction, occupying the interstices among the cation, as shown in Figure 7.

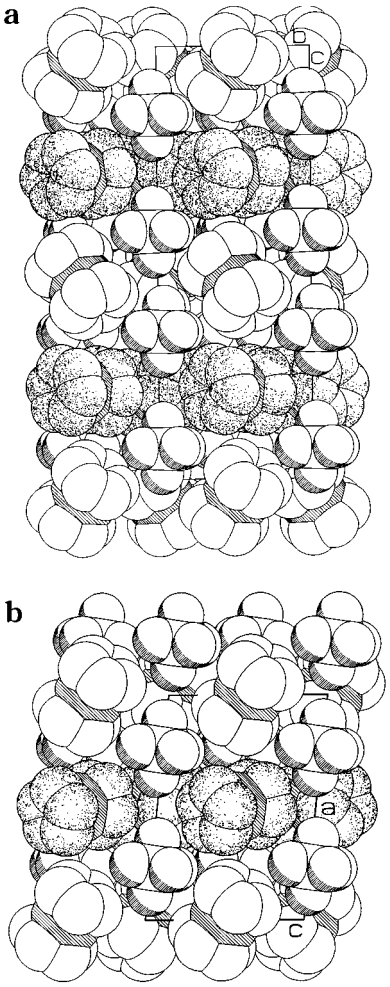

Figure 5. Comparison of the space-filling representation of **3** with the corresponding orientation of **1** in its form II. Note how the cations belonging to different layers have similar relative orientations although the stacking periodicity is A/B/A/B in **1** and A/B/A′/B′/A/B in **3**.

Database Analysis and the Importance of Charge-Assisted C−H---F Interactions. Since the peripheral atoms in systems **1**−**4** are only of two types, namely H and F, and the H-atoms are bound only to carbon, these crystals can be used to test the role of C−H---F(-P) interactions in controlling crystal stability and cohesion. Interactions of this kind are expected to be weak because of the low acidity of the C−H system. However, the number of potential donors and acceptors is very large (compared with compounds carrying conventional strong donors such as −COOH, −OH, etc.) and may well result in an important *collective* contribution to cohesion.

Furthermore, weak hydrogen bonds, such as C−H---O bonds, can be strengthened *via* charge as-

(12) (a) Braga, D.; Grepioni, F. *Organometallics* **1991**, *10*, 1254. (b) Braga, D.; Grepioni, F. *Organometallics* **1991**, *10*, 2563.

(13) Packing coefficients are obtained from the ratio p.c. = $[[V_{anion} + V_{cation}](Z/V_{cell})]$ where *Z* is the number of formulas in the unit cell, V_{cell} is the cell volume, and V_{anion} and V_{cation} are the volumes of the anions and cations evaluated by the integration method; see: Gavezzotti, A. *J. Am. Chem. Soc.* **1983**, *95*, 5220.

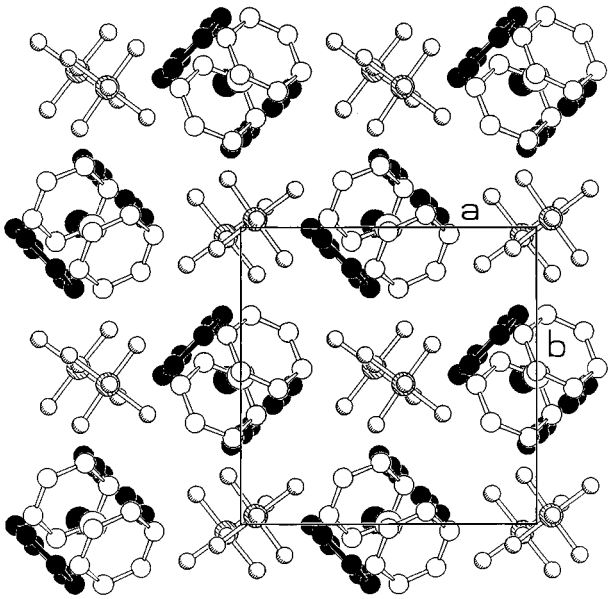

Figure 6. Schematic representation of the cation arrangement in **3**. Note how the Bz−Cr−Bz axes are staggered in projection as in the low-temperature phase of **1** and **2**.

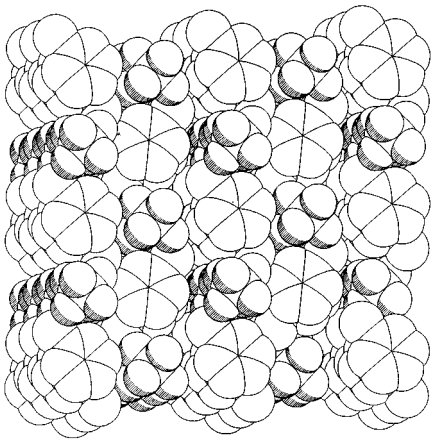

Figure 7. Molecular packing of compound **4**: space-filling representation of the cation and anion columns extending parallel to the *a*-axis. H atoms are omitted for clarity.

sistance.[14] Stronger C−H---O bonds are, of course, more interesting in crystal engineering applications. Charge assistance is "naturally" provided in organometallic salts if the donor is charged positively and the acceptor is charged negatively. This is, for instance, the case of the organic−organometallic supramolecular Cr and Co aggregates with cyclohexanedione and organic acids recently described.[14,15] The stability of these crystalline materials is largely due to interactions of the $O-H---O^{(-)}$ type between the organic moieties and of the $C-H^{(\delta+)}---O^{(\delta-)}$ type between the organometallic cations and the anionic organic frameworks. In approaching C−H---F interactions in this study we wondered if a similar role could be ascribed to interactions of the $C-H^{(\delta+)}---F^{(\delta-)}$ type between organometallic cations and the fluorine atoms of the PF_6^- anions. The PF_6^- anion is one of the most common anions used to precipitate and crystallize organometallic and inorganic cations.

(14) (a) Braga, D.; Costa, A. L.; Grepioni, F.; Scaccianoce, L.; Tagliavini, E. **1997,** *16,* 2070. (b) Braga, D.; Angeloni, A.; Grepioni, F.; Tagliavini, E. *J. Chem. Soc., Chem. Commun.* **1997**, 1447.

(15) Braga, D.; Angeloni, A.; Grepioni, F.; Tagliavini, E. *Organometallics*, in press.

In order to put the analysis in a broad perspective, we have analyzed the data available in the CSD and searched for intermolecular H-bonds of the $X-H---F^{(\delta-)}$ type (X = C, N, O see the Experimental Section). For X = C, two separate searches were carried out. In the first, only C−H fragments for which the C atom is directly bound to the metal atom were considered (149 compounds), in order to compare the result of the search directly with the hydrogen-bonding parameters calculated for our compounds **1**−**4**. In the second one no restrictions were applied to the C atom (831 compounds). Interactions of the $N-H---F^{(\delta-)}(P)$ and $O-H---F^{(\delta-)}(P)$ types were also screened (80 and 15 compounds, respectively).

Our attention to the problem of $X-H---F^{(\delta-)}$ interactions was also attracted by the recent study of the participation of organic fluorine in intermolecular hydrogen bonds reported by Dunitz and Taylor.[16] These authors have convincingly demonstrated, by means of a database analysis and of theoretical calculations, that fluorine when covalently bound to carbon does not frequently form hydrogen bonds with conventional hydrogen bond donors, including O−H, N−H, and C−H groups.

The results of our analysis, which is confined to inorganic fluorine bound to phosphorous in PF_6^- anions, are summarized in the scattergrams shown below in Figures 8 and 12, where $X-H---F^{(\delta-)}(P)$ angles (X = C, N, O) are plotted against the $(X)H---F^{(\delta-)}(P)$ distances. Although the sample population is very different in the four cases, all types of interactions follow the normal trend observed for hydrogen bonds, *i.e.*, as the distance between hydrogen and acceptor atoms decreases, the X−H---F vectors becomes straighter and the bond approaches linearity.[17] Besides this general behavior, there is a large number of bonds that fall below the van der Waals cutoff distances and are clearly indicative of specific and directional interactions involving donors and acceptors. Some key examples extracted from the three searches will be discussed below.

The two scattergrams of $(C)H---F^{(\delta-)}(P)$ interactions (Figure 8a,b) show no appreciable difference; *i.e.*, there is no appreciable effect of the direct bonding to transition metal atoms on the geometry of the interaction. This is confirmed by the histograms of $(C)H---F^{(\delta-)}(P)$ separations (Figure 8c,d), which show that, in spite of the much larger number of salts in the general search (831 *versus* 149 compounds), the two populations have the same distribution. The percentage of contacts falling, for example, in the range 2.00−2.32 Å is 10% in both cases. It can be observed that, as the H---F distance moves toward shorter values, the distribution of $C-H---F^{(\delta-)}(P)$ angles, which covers the range 110−180°, concentrates in an area of higher angular values. Most short $(C)H---F^{(\delta-)}(P)$ interactions, on the other hand, involve metal-coordinated cyclopentadienyl and arene ligands, which are also the most common donors

(16) Dunitz, J.; Taylor, R. *Chem. Eur. J.* **1997**, *3*, 89.

(17) (a) Bernstein, J.; Davis, R. E.; Shimoni, L.; Chang, N.-L. *Angew. Chem., Int. Ed. Engl.* **1995**, *34*, 1555. (b) Bernstein, J.; Etter, M. C.; Leiserowitz, L. In *Structure Correlation*; Bürgi, H.-B., Dunitz, J. D., Eds.; VCH: Weinheim, 1994; p 431. (c) Taylor, R.; Kennard, O. *J. Am. Chem. Soc.* **1982**, *104*, 5063. (d) Allen, F. H.; Kennard, O.; Taylor, R. *Acc. Chem. Res.* **1983**, *16*, 146. (e) Jeffrey, G. A.; Saenger, W. *Hydrogen Bonding in Biological Structures*; Springer-Verlag: Berlin, 1991.

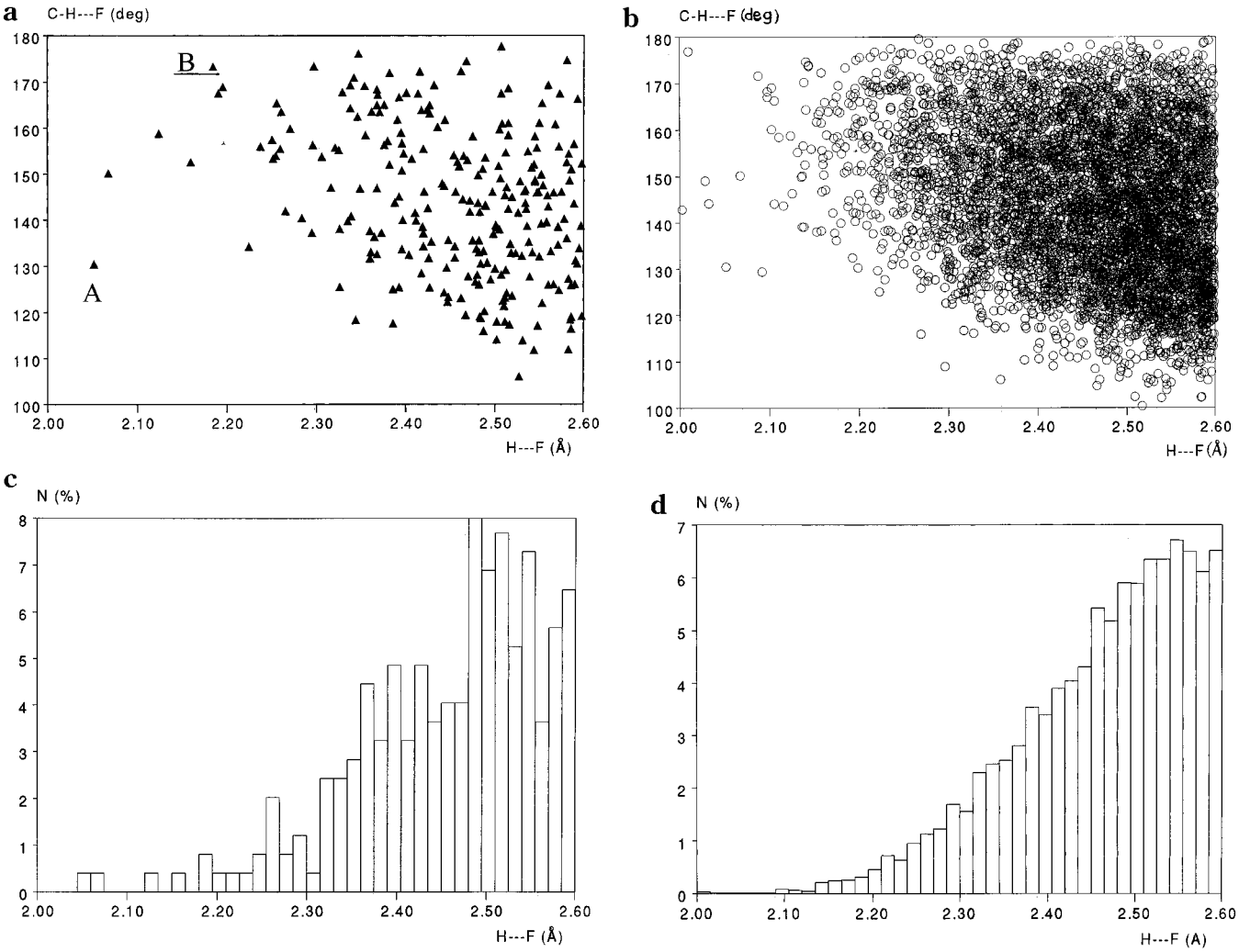

Figure 8. Scattergrams of C−H---F$^{(\delta-)}$(P) angles *versus* (C)H---F$^{(\delta-)}$(P) distances and histograms of (C)H---F$^{(\delta-)}$(P) distances for C-atoms directly bound to transition metal atoms (a, c) and for "any" C−H (b, d).

in hydrogen bonds involving CO ligand acceptors.[18] The fact that the two types of interactions, namely (C)H---O(C) and (C)H---F$^{(\delta-)}$(P) interactions, span the same distance range suggests that fluorine in PF_6^- has a basicity very similar to that of CO. The similarity between the CO ligand and the PF fragment as acceptors is also in the tendency to multiple interactions as will be shown below.

The information on (C)H---F$^{(\delta-)}$(P) interactions in crystalline **1**−**4**, at low and room temperatures, is summarized in Table 3. In both form I and form II of **1** and **2** there is a large number of C−H---F interactions shorter than 2.6 Å between the C_5H_5 ligands and the PF_6^- anions. There is good agreement with the distribution shown in Figure 8a. In particular, it is noteworthy that there are, respectively, two and five C−H---F distances between 2.3 and 2.4 Å in form I and form II of **2**, while all links are above 2.42 Å in crystals of **1**. Distances as short as 2.3 are otherwise observed in crystalline **3**. Whether these differences reflect the effect on the C−H acidity of the metal atoms (Co in **1**, Fe in **2**, Cr, in **3**) is difficult to state with confidence. One may speculate, however, that shorter and more numerous C-H---F distances are present in **3**, which does not undergo a phase change, and in **2**, for which the stability of the intermediate phase is much larger than in **1**. A perspective view of the pattern of C−H---F interactions along the *c*-axis is shown in Figure 9.

We have chosen to show two examples taken from the restricted search: the first is compound $[(C_6H_5Me)W(H)_2(PMe_3)_3][PF_6]$[19a] (A in Figure 8a), which represents the shortest interaction; the second is the one showing, in the interval of distances below 2.20 Å, the angular value closest to 180°, $[(C_6H_5F)_2W(H)][PF_6]$[19b] (B in Figure 8a). In crystalline $[(C_6H_5Me)W(H)_2(PMe_3)_3][PF_6]$, a fluorine atom is involved in a bifurcated interaction with two hydrogen atoms belonging to the toluene ligands of two neighboring tungsten cations (see Figure 10). $[(C_6H_5F)_2W(H)][PF_6]$ is relevant for our discussion because its molecular formula is quite similar to those of the compounds reported in this paper. One fluorine atom of the PF_6^- anion participates in a bifurcated interaction with two H atoms of the aromatic

(18) (a) Braga, D.; Grepioni, F.; Biradha, K.; Pedireddi, V. R.; Desiraju, G. R. *J. Am. Chem. Soc.* **1995**, *117*, 3156. (b) Braga, D.; Grepioni, F. *Acc. Chem. Res.* **1997**, *30*, 81.

(19) (a) Green, M. L. H.; Hughes, A. K.; Lincoln, P.; Martin-Polo, J. J.; Mountford, P.; Sella, A.; Wong, L.-L.; Bandy, J. A.; Banks, T. W.; Prout, K.; Watkin D. J. *J. Chem. Soc., Dalton Trans.* **1992**, 2063. (b) Prout, K.; Gourdon, A.; Couldwell, C.; Meunier, B.; Miao, F. M.; Woolcock, J. *Acta Crystallogr. Sect. B* **1982**, *B38*, 456.

Table 3. Hydrogen-Bonding Parameters for Compounds 1−4

compd	C(H)---F$^{(\delta-)}$(P) (Å)	(C)H---F$^{(\delta-)}$(P) (Å)	C-H---F$^{(\delta-)}$(P) (°)
1 (form I)	3.245	2.441	130.3
	3.427	2.425	153.8
	3.399	2.548	135.0
	3.422	2.536	138.6
	3.437	2.573	136.4
	3.339	2.584	126.4
	3.266	2.439	132.4
1 (form II)	3.310	2.450	135.8
	3.488	2.450	160.7
	3.355	2.451	140.5
	3.436	2.523	141.6
	3.235	2.448	128.7
	3.626	2.582	162.5
	3.182	2.451	123.9
2 (form I)	3.371	2.372	153.2
	3.185	2.390	129.2
	3.542	2.535	154.9
	3.112	2.576	109.8
	3.222	2.489	124.2
	3.404	2.405	153.2
	3.352	2.520	133.1
2 (form II)	3.253	2.396	135.3
	3.394	2.373	157.2
	3.291	2.363	143.1
	3.384	2.579	130.7
	3.414	2.488	143.2
	3.234	2.501	124.3
	3.178	2.399	127.9
	3.639	2.593	162.9
	3.079	2.329	125.0
3	3.435	2.548	138.9
	3.233	2.320	141.2
	3.322	2.455	136.4
	3.567	2.519	163.3
	3.539	2.480	166.4
	3.357	2.489	136.6
	3.417	2.404	155.7
	3.380	2.301	177.5
	3.137	2.420	122.6
	3.472	2.542	143.7
	3.353	2.303	163.4
	3.406	2.543	136.2
	3.327	2.497	132.8
4	3.371	2.399	149.0
	3.401	2.534	136.6
	3.303	2.519	128.6

rings of a neighboring cation, while four other fluorine atoms are involved in short pairs of interactions with two additional cations related by translational symmetry (see Figure 11). It is interesting to note that the shortest separation between the fluorine atoms covalently bound to the C_6 rings and the hydrogen atoms on an adjacent cation are quite long (2.764 and 2.597 Å). This observation is in keeping with the observation discussed by Dunitz and Taylor[17] that organic fluorine, covalently bound to carbon, does not commonly form hydrogen bonds. Importantly, however, the same authors pointed out that when the fluorine atom is part of an anion like, for example, the fluorobenzoate anion, it can become "unusually electron rich" and a good acceptor in hydrogen bonding. Clearly, this is the case of the F-atom in PF_6^- anions.

As mentioned above, N−H---F$^{(\delta-)}$(P) and O−H---F$^{(\delta-)}$(P) interactions show the same distribution as C−H---F$^{(\delta-)}$(P) interactions. The two searches have been carried out with no restriction on the geometry of the N−H and O−H fragments; *i.e.*, they were not requested to be directly bound to the metal center. The

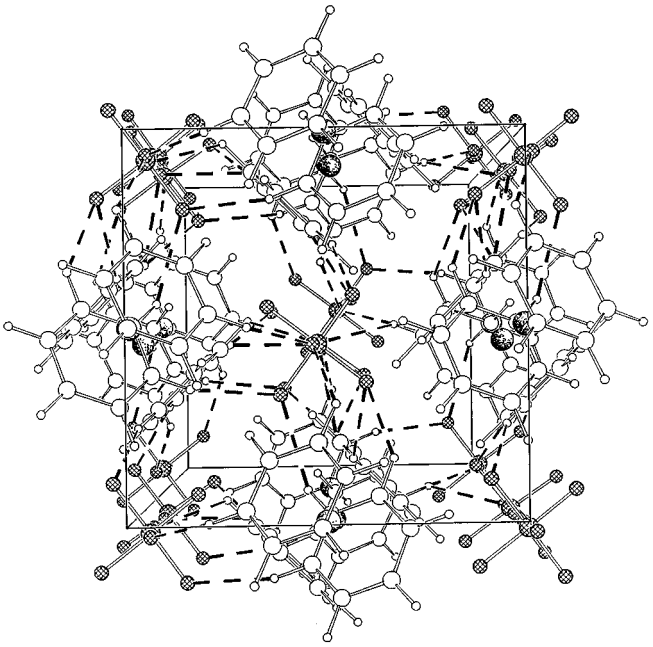

Figure 9. Perspective view along the *c*-axis of the pattern of (C)H---F$^{(\delta-)}$(P) interactions in compound **3**.

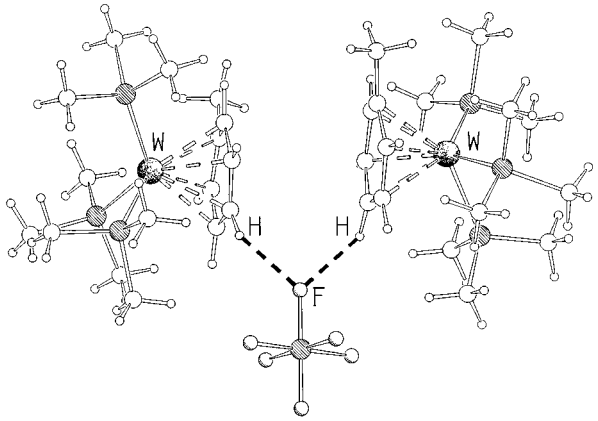

Figure 10. (C)H---F$^{(\delta-)}$(P) interactions in crystalline $[(C_6H_5Me)W(H)_2(PMe_3)_3][PF_6]$ (A in Figure 8a): a fluorine atom is involved in a bifurcated interaction with two hydrogen atoms belonging to the toluene ligands of two neighboring tungsten cations.

results are shown in Figure 12a, for O−H and N−H donors, respectively. Both scattergrams resemble quite closely the ones obtained for the carbon atom (see Figure 8), although in the case of oxygen the number of hits is scarce and constituted mainly of compounds in which the O−H fragment belongs to water molecules, present as crystallization solvent or as a metal-coordinated ligand.

Two examples have been selected from these searches and are briefly discussed below. The interaction network in crystalline [(5-Me-4,6-diaza-2,8-diazonio-nona-2,4,7-triene-3,7-diyl)Fe(H)$_2$(CNMe)$_4$][PF$_6$]$_2$[20a] (A in Figure 12a) is shown in Figure 13. The cation and the anion form a dimeric pair *via* two short hydrogen bond interactions involving two fluorine atoms of the same anion and two hydrogen atoms belonging to an N−H

(20) (a) Rojo, T.; Cortes, R.; Lezama, L.; Mesa, J. L.; Via, J.; Arriortua, M. I.; *Inorg. Chim. Acta* **1989**, *165*, 91. (b) Castro, J. M.; Hope, H. *Inorg. Chem.* **1978**, *17*, 1444.

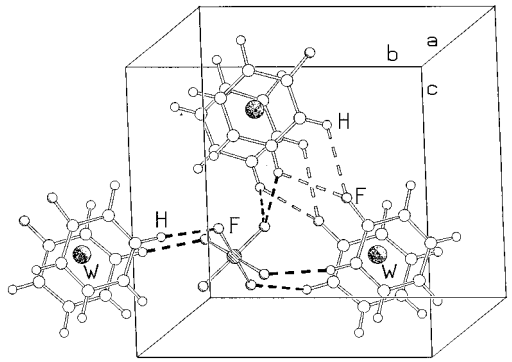

Figure 11. (C)H---$F^{(\delta-)}$(P) interactions in crystalline $[(C_6H_5F)_2W(H)][PF_6]$ (B in Figure 8a): a total of five fluorine atoms of the PF_6^- anions participate in multiple interactions (broken filled bonds) that are shorter than those involving the organic fluorine atoms carried by the ligands (broken empty bonds).

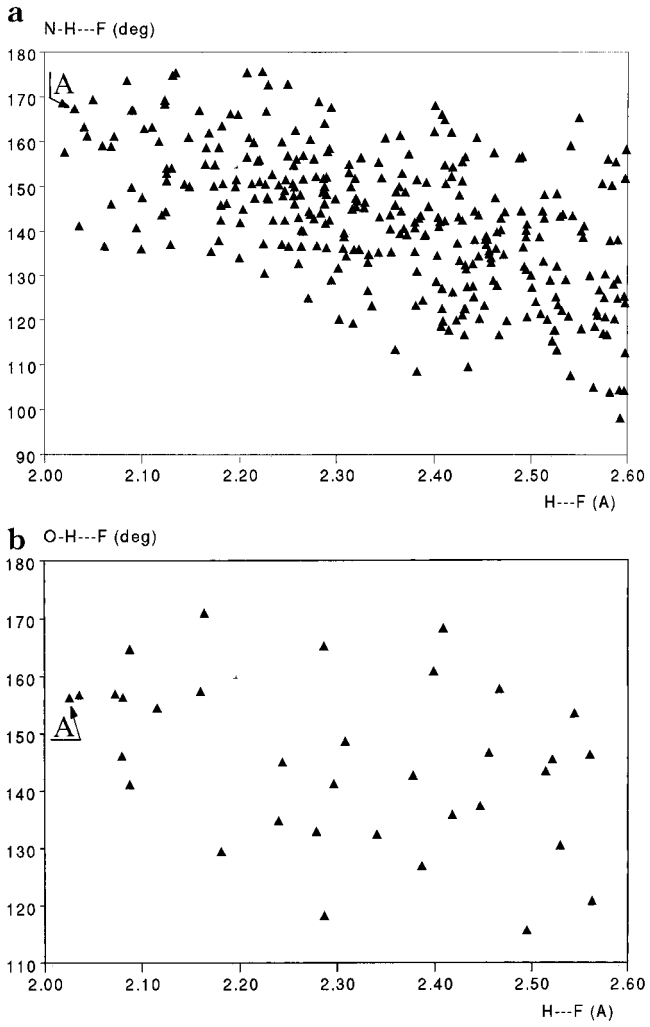

Figure 12. Scattergrams of (X)H---$F^{(\delta-)}$(P) distances plotted against X−H---$F^{(\delta-)}$(P) angles: X = N (a), X = O (b).

and a methyl group on the cation. The interaction network in crystalline [(terpyridine)Cu(H_2O)(NCO)]-$[PF_6]$[20b] (A in Figure 12b) is depicted in Figure 14. Two anions and two copper cationic complexes form a dimeric unit held together by short O−H---F interactions, involving the water molecules coordinated to the Cu atoms, and by C−H---F interactions involving H atoms

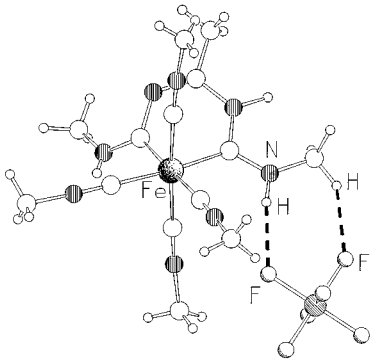

Figure 13. (a) Hydrogen bonds of the (N)H---$F^{(\delta-)}$(P) type in crystalline [(5-Me-4,6-diaza-2,8-diazonio-nona-2,4,7-triene-3,7-diyl)Fe$(H)_2(CNMe)_4][PF_6]_2$ (A in Figure 12a). The cation and the anion form a dimeric pair *via* two short (N)H---$F^{(\delta-)}$(P) hydrogen-bond interactions.

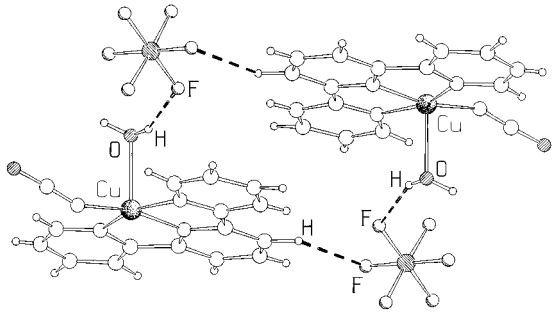

Figure 14. Hydrogen bonds of the (O)H---$F^{(\delta-)}$(P) type in crystalline [(terpyridine)Cu(H_2O)(NCO)][PF_6]. Two anions and two copper cationic complexes form a dimeric unit held together by short O−H---F interactions involving two metal-coordinated water molecules.

of the terpyridine group and a second different fluorine atom of the same anions.

Conclusions

We have attempted with this paper to bring together different issues of solid state chemistry, dynamics, and crystal engineering. The major outcomes of this study can be summarized as follows:

(i) Crystalline $[(C_5H_5)_2M][PF_6]$ (M = Co and Fe) are remarkable structural systems. Both crystals are able to *switch* reversibly between three phases, two of which are fully ordered. The stability of the intermediate room temperature phase (form I) differs in the two salts by ca. 75° in the case of Co and 134° in the case of Fe.

(ii) The high-temperature phase (form III) is, at least in the case of cobalt, related to the room-temperature phase, and the whole phase transitional behavior can be seen as a progressive adjustment of the crystal structure to the dynamical requirements of the globular cations that occupy more space as the temperature increases.

(iii) Crystalline **1** is remarkably robust so that the phase transitions can be followed on the single crystal diffractometer and diffraction data of the different phase can be collected on the same crystal specimen.

(iv) Form III of **1** can be described either as a *semi*-plastic cubic crystal in which the cobalticinium cations have lost long-range order and occupy the center of a "box" defined by ordered PF_6^- anion or as a monoclinic

crystal (with the *b*-angle close to 90°) in which the cations show different extent of orientational disorder over two crystallographic independent sites. This latter model has the advantage of providing a path for returning to the nondegenerate ordered distribution of form II on cooling the crystal.

(iv) The chromium analogue **3**, in spite of the difference in molecular structure, crystallizes in a manner that is strictly related to that of the low-temperature phases of **1** and **2** and does not undergo phase changes on cooling. When benzene is replaced with toluene, the architecture of **1**−**3** is no longer compatible with the cation shape, and the crystal structure of **4** is based on cationic columns.

(v) The four crystalline materials present a large number of short C−H---$F^{(\delta-)}$(P) interactions between the cyclopentadienyl (**1** and **2**) or the arene ligands (**3** and **4**) and the PF_6^- anions. The length and number of short distances correlates with the position of the metal atom in the Periodic Table; *i.e*, more numerous and shorter C−H---$F^{(\delta-)}$(P) distances are in the order $(C_6H_6)_2Cr^+$ > $(C_5H_5)_2Fe^+$ > $(C_5H_5)_2Co^+$, which is also the order of increasing need of back-donation from the metal atoms onto the ligands.

(vi) The Cambridge Crystallographic Database contains 926 coordination and organometallic salts crystallized with the PF_6^- anion with (X)H---$F^{(\delta-)}$(P) distances shorter than 2.6 Å (831 for X = C, 80 for X = N, 15 for X = O). The distribution of distances and angles are in all three cases indicative of hydrogen-bonding behavior. There are many short interactions, and as the distance decreases the X−H---$F^{(\delta-)}$(P)angle approaches linearity. When the donor is carbon, the behavior recalls very closely that previously found in C−H---OC interactions involving the CO ligand.

(vii) Both our experimental results and the abundant information available in the CSD concur to indicate that the inorganic fluorine atom in PF_6^- forms weak hydrogen bonds with a variety of donors. With respect to organic fluorine, the X−H---$F^{(\delta-)}$(P) interaction is "charge assisted", i.e., the weak interaction is seemingly reinforced by the different ionic charge carried by anion and cations.

The hydrogen bond provides the most efficacious and robust noncovalent infrastructure to complex architectures and, for this reason, is being widely employed in these days of supramolecular chemistry and crystal engineering. The interaction is basically electrostatic in nature; hence, all factors influencing the charge distribution on the donor/acceptor system affect the strength of the hydrogen bond. Owing to the relevance of organometallic ions, the role of ionic charge in organometallic and inorganic crystal engineering is much more relevant than in organic chemistry.

Acknowledgment. D.B. and S.D. gratefully acknowledge CIBA-Geigy for an ACE fellowship and the ERASMUS exchange program "Crystallography" (N.S.). We thank anonymous reviewers for useful comments and suggestions. Financial support from the University of Bologna - Project "Intelligent Molecules and Molecular Aggregates" (D.B. and F.G.) is acknowledged.

Supporting Information Available: Tables of anisotropic thermal parameters and fractional atomic coordinates, a complete list of bond lengths and angles, ORTEP drawings, and input files for the CSD searches (26 pages). Ordering information is given on any current masthead page.

OM9706626